INCORPORATING A LOCALLY ESTIMATED APPEARANCE MODEL IN THE GRAPH-CUTS ALGORITHM TO EXTRACT SMALL HEPATIC VESSELS

Neda Sangsefidi[a], Amir Hossein Foruzan[a], Ardeshir Dolati[b], Yen-Wei Chen[c].

[a]Department of Biomedical Engineering, Engineering Faculty, [b]Department of Mathematics and Computer Science, Science Faculty, Shahed University, Tehran, Iran.
[c]Intelligent Image Processing Lab, College of Information Science and Engineering, Ritsumeikan University, Shiga, Japan.

ABSTRACT

In this paper, we incorporate a locally estimated appearance model to enrich the data term of the graph-cuts algorithm. It balances between data term and smoothing terms in order to extract small liver vessels. We estimate stochastic parameters of vessel and liver tissues using the MIP image. Medial axes of the vessels are then enhanced by a multi-scale filter. The skeleton of the axes are used to prepare the appearance model which is employed to prepare s-link weights in the graph-cuts algorithm. We evaluated the proposed method quantitatively using public synthetic data and qualitatively using clinical images. We obtained an average Dice measure of 0.93 which was comparable to recent researches. We achieved segmentation of liver vessels up to the fourth order too.

Index Terms— Hepatic vessels, graph-cuts algorithm, vessel segmentation, CT liver images.

1. INTRODUCTION

Prior knowledge about the locations and structure of hepatic vessels is vital for quantification of vascular diseases and liver/vessel treatment planning [1]. In contrast-enhanced CT images, extraction of liver vessels is a challenging task due to reduced concentration of contrast-media in small branches, bifurcations, different vessel widths, image noise, and existence of pathological structures.

A major class of hepatic vessel extraction methods is feature-based techniques in which a feature map is formed and a classification algorithm divides image elements into vessel/non-vessel pixels. Hessian-based approaches (including the popular Frangi filter [2]) and graph-cuts methods are among feature-based techniques [2-5].

Marcan *et al.* developed a robust method against different MRI imaging protocols [6]. They employed the Frangi filter and region-growing to segment liver vessels. To improve the results, they employed morphological filters. Wang *et al.* used the Frangi filter to enhance tubular structures and utilized a graph-based algorithm to extract and delineate portal and hepatic veins [7]. In 2015, the authors proposed an algorithm to extract hepatic arteries [8]. They enhanced an input image by the Frangi filter and initially segmented the arteries using a Bayesian classifier. To connect the gaps between vessel segments, they utilized both directional morphological filters and the minimum cost path technique.

Cheng *et al.* addressed segmentation of thin vessels and vessels attached to each other or to pathological structures [9]. Initially, they enhanced vessels by a multi-scale filter and extracted their medial axes. They formed the boundaries of vessels by a model-based scheme and then improved them by a parametric active contour under shape and size constraints. To segment vessels up to the third order, Luu *et al.* obtained the histogram of an input image to find an optimum threshold. The threshold was later used to define seeds for a region-growing algorithm [10]. Chen *et al.* employed the Frangi filter, post-processed the results by region-growing algorithm, and used morphological filters to fill the gaps and to extract hepatic veins. In a recent research, Lu *et al.* addressed the problem of noise in extraction of hepatic vessels in MRI data [11]. A user provided seed points and statistical feature vectors were prepared as the balloon force for contour evolution in a variational framework.

Regarding graph-cuts techniques for vessel extraction, Wankhede *et al.* used conventional graph-cuts energy function for segmentation of retinal blood vessel [5]. Chen *et al.* addressed segmentation of low-contrast small liver vessels [12]. They employed the quick-shift clustering technique to define super-pixels. Then, they applied the quick shift and graph-cuts algorithm iteratively to segment small vessels. Zhai *et al.* dealt with memory and computational challenges of the graph-cuts segmentation [4]. They included the output of the Frangi filter as the shape feature and intensity data as the appearance feature in the graph-cuts data term. They also used a sparse matrix to deal with memory requirements.

Feature-based approaches have difficulties in segmentation of small and low-contrast vessels [13]. The Hessian-based methods have also low responses at bifurcations and vessel boundaries [4]. If the parameters of the algorithm are tuned to include higher order of the vascular branches, considerable over-segmentation will happen. Interruption of

the contrast-media along the end branches results in small segments which should be fixed by a connectivity algorithm. Most of these methods have been applied on normal datasets and pathological cases have been ignored.
Regarding vessel segmentation using the graph-cuts technique, the smoothness term of the cost function makes small vessels neglected in the segmentation process. To represent intensity variations of the vessels, a single static model has been employed in the data term. Therefore, small thin vessels are not segmented accurately since the summed cost of the cuts along the boundary is higher than the cost across the vessel [14].

In our previous work, we proposed a Hessian-based vessel extraction technique [15]. In this paper, we consider extraction of end branches in contrast-enhanced CT images of liver. We consider both normal and pathological cases. We extract up to the fourth order branches using a modified graph-cuts technique. Instead of a static appearance model, we introduce a dynamic model in which the parameters of the model are defined locally. This helps to leverage t-link weights compared to n-link weights in small low-contrast vessels. As another innovation, we define a tubular ROI in which the graph-cuts technique is applied. Therefore, the run-time of our method is reduced considerably.

2. THE PROPOSED METHOD

After preprocessing an input CT volume, statistical parameters of both liver and vessels are estimated. To accurately estimate the stochastic parameters, we employ Maximum Intensity Projection (MIP) of the input image. Next, we employ these parameters to threshold the CT volume to remove some of non-vessel voxels. This step is crucial for the success of next stage (medial axis enhancement). An accurate vascular appearance model greatly influences the results of the graph-cuts segmentation. To construct an appearance model of hepatic vessels, the most insured region is the central voxels of a vessel. Therefore, we enhance medial axes of vessels and find the skeleton of the axes. In each region, we fit a Gaussian function to the local data and calculate the model parameters using Maximum Likelihood estimation. Next, we prepare the t-link and n-link weights of the graph corresponding to the input image. The minimum cut of the graph is found as the output of the algorithm and it is used as the segmentation result.

2.1. Preprocessing

Initially, an input CT image containing the abdominal region and the mask of the liver are read. In the mask image, liver and non-liver voxels are labeled as one and zero respectively. To increase the contrast between vessels and liver tissue, a contrast-media is injected to the patient before acquisition of the image. The mask image is used to define the ROI of the liver. Definition of the ROI reduces the size of the input image up to 30% of its original size and helps our code to run faster. At the end of this step, we employ Anisotropic Diffusion Filter (ADF) to reduce image noise.

5.1. Estimation of tissues statistical parameters

To estimate statistical parameters of liver and vessel, we employ the Gaussian mixture model. Since voxels containing liver vessels comprise a small number of the total image elements, vessel parameters are not accurately estimated by simply fitting the model to the 3D image. Based on our experience, we fit the model to the MIP of the image in which vessels have a considerable proportion of the image elements (Fig. 1a).

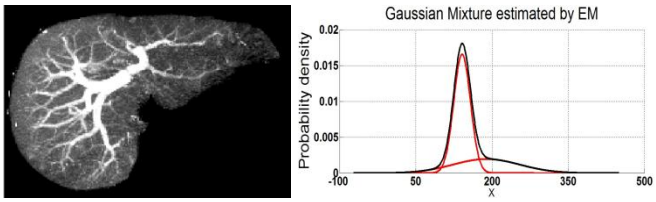

(a) (b)

Fig. 1 - (a) The MIP of a typical image. (b) The results of the Gaussian mixture model fitting.

After obtaining statistical parameters, we threshold the input image in the range $[\mu_L - \sigma_L,\ \mu_V + \sigma_V]$ where μ_L and σ_L are mean and standard deviation of liver intensities and μ_V and σ_V are mean and standard deviation of vessel intensities respectively. After thresholding, some non-vessel pixels are removed (Fig. 2a).

2.2. Extraction of Vascular Medial axes

We enhance medial axes of the vessel and extract the skeleton of the enhanced axes. We employ the algorithm proposed by Pock *et al.* [16] to enhance medial axes of both large and small vessels. Similar to the popular algorithm proposed by Frangi *et al.*, the method of Pock is a robust technique for medial axis enhancement. The Pock's method enhances central part of the vessel; however, the Frangi's method improves intensities of both central part and the neighboring regions. Since we have to estimate the statistics of medial axes accurately, the Pock's method is more appropriate to our needs. To consider vessels with different widths, the input image is smoothed by a Gaussian filter ($I^{(\sigma)}$) with different variances (σ^2). In each scale, the Hessian matrices of the image voxels are calculated. At each voxel, the eigenvectors of the Hessian matrix define the main directions of the image objects. The second and third vectors (V_2 and V_3) are used to construct a rotating phasor ($V_\alpha = \cos(\alpha)\, V_2 + \sin(\alpha)\, V_3$). The phasor is rotated from V_2 to V_3 and then to $-V_2$. The profile of the image gradient ($\left|\nabla I^{(\sigma)}\right|$) is resampled in the direction of the phasor. The initial medialness (R_0) of a typical point X is defined as the average of N gradient samples in location $X + \rho V_\alpha$ (Eq. 1).

$$R_0 = \frac{1}{N}\sum_{i=0}^{N-1}\left|\nabla I^{(\sigma)}(X + \rho V_\alpha)\right| \qquad \text{(Eq. 1)}$$

In Eq. (1), ρ is a constant which depends on the scale of the image. A weighted average of R_0 is used as the medialness of the image. The result of medial axes enhancement of a typical image is shown in Fig. 2b. We change the scale parameter from 0.1 to 6 in steps of 0.5. We apply a threshold on the output of the Pock method to obtain a binary image. To remove trivial objects, morphological filters are employed to eliminate objects smaller than 10 pixels.

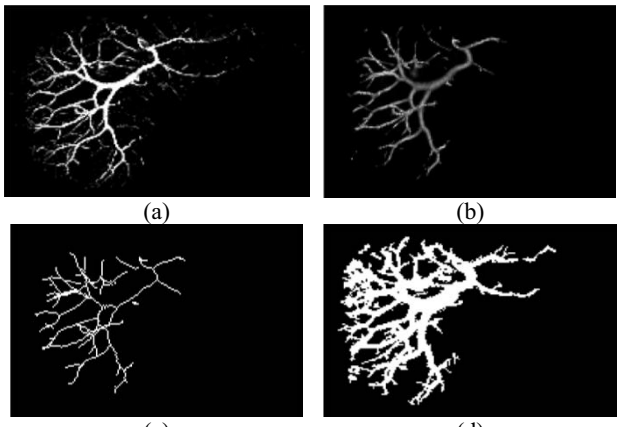

(a) (b) (c) (d)

Fig. 2 – (a) Thresholded input image. (b) Enhanced medial axes. (c) Extracted skeleton. (d) Output of the proposed method.

We extract the medial axes of the vascular tree from the cleaned binary object. We employ the method of Lee *et al.* [17] to achieve accurate skeletons of the vessels. The skeleton algorithm is not sensitive to noise and preserves topology of objects. The skeletons define the central region of the vessels. Next, we obtain the appearance models.

2.3. Modified Graph-cuts Segmentation

The graph-cuts algorithm introduced by Boykov *et al.* has already been used for segmentation of medical images including vascular extraction [18]. It obtains global minimum of an energy function (E_T) consisting of data (E_{Data}) and smoothness ($E_{boundary}$) terms. The data term represents the probability that a voxel belongs to object or background. In conventional graph-cuts, a global model is employed for coding object and background. In small vessels and low-contrast regions, the model is not a good representation of the cases. Therefore, E_{Data} has a high value in these regions and they are labeled as background. In this research, we replace the data term by a local energy term (E_{Local}) to balance the total energy in small vessels and low contrast regions (Eq. 2).

$$E_T = E_{Local} + E_{boundary} \qquad \text{(Eq. 2)}$$

We consider a global model for the background voxels and a locally estimated model for object elements. The model is a Gaussian function which we have to estimate its mean and variance. Estimation of the local stochastic model is performed by the maximum likelihood method. The most confident data for doing estimation is the medial axes of the vessels. The skeleton of the vessels are used to build the model.

For a pixel P on the skeleton of the vessels (S), its $5 \times 5 \times 5$ neighbors ($N(P)$) are selected and their corresponding intensities in the image (I) are used to estimate local mean (m_P) and variance (σ_P^2) of the statistical model (Eq. 3-4).

$$m_P = \frac{\sum_{i \in N(P)} I(i) \times S(i)}{\sum_{i \in N(P)} S(i)}, \quad P \in S. \qquad \text{(Eq. 3)}$$

$$\sigma_P^2 = \frac{\sum_{i \in N(P)} [I(i) \times S(i) - m_P]^2}{\sum_{i \in N(P)} S(i) - 1}, \quad P \in S. \qquad \text{(Eq. 4)}$$

The parameters of the model are stored in the position P. The appropriate profile model of a vessel in voxel X is the model corresponding to the nearest skeleton point (Eq. 5).

$$m_X = m_{\hat{P}}, \quad \sigma_X^2 = \sigma_{\hat{P}}^2, \qquad \hat{P} = \underset{P}{argmin}(|X - P|) \qquad \text{(Eq. 5)}$$

In the graph-cuts algorithm, the links connecting the point X to the source terminal (W_S), the sink terminal (W_T), and to a neighboring point N_X (W_n) are defined as in Eqs. 6-8.

$$W_S(X) = exp\left[-\frac{(I(X) - m_X)^2}{2\sigma_X^2}\right]. \qquad \text{(Eq. 6)}$$

$$W_T(X) = exp\left[-\frac{(I(X) - m_{bk})^2}{2\sigma_{bk}^2}\right]. \qquad \text{(Eq. 7)}$$

$$W_n(X, N_X) = \frac{1}{1 + |I(X) - I(N_X)|}. \qquad \text{(Eq. 8)}$$

Finally, we apply the graph-cuts algorithm and segment the vascular tree.

3. RESULT AND DISCUSSIONS

We evaluated the proposed method by synthetic and clinical data. The synthetic data belonged to VascuSynth [19-20]. It contained randomly generated images with small and large bifurcations. Since the gold standard mask was available for this dataset, we used it for quantitative evaluation. The evaluations were performed using True Positive Rate (TPR) and Dice metrics defined in Eqs. 8-9.

$$TPR = \frac{|A \cap M|}{|M|}. \qquad \text{(Eq. 8)}$$

$$Dice = \frac{2|A \cap M|}{|A| + |M|}. \qquad \text{(Eq. 9)}$$

In Eqs. 8-9, A and M refer to segmentation result of our method and manual segmentation respectively and $|\cdot|$ is the size operator.

The clinical data included the portal-venous phase of contrast-enhanced CT images of the abdominal region. They belonged to Osaka University, Japan and contained 16 abdominal images of the portal venous phase data. The resolution and size of images were 512×512×159 and

$0.625 \times 0.625 \times 1.25$ mm^3 respectively. The usage of this set was approved by the University Ethics Committee.

Except for the graph-cuts algorithm, we implemented the remaining parts of the code in MATLAB environment. The graph-cuts algorithm was built using the Boykov–Kolmogorov's C++ implementation [18]. The code was run on a personal computer with Intel® Core™ -i7 (2.20GHz) with 8 GB RAM running 64-bit Windows 7.

3.1. Validation on Synthetic Data

We quantitatively evaluated our method using synthetic data. We added Gaussian noise to the input image to evaluate sensitivity of the proposed algorithm with noise. Variance of noise was changed from 1% to 10% (Fig. 3).

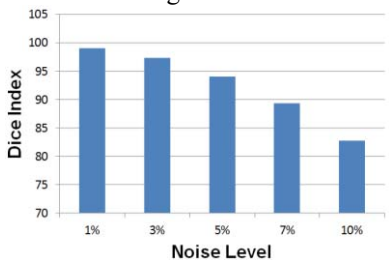

Fig. 3 – Evaluation of the proposed method using Dice measure.

Averages of the Dice and TPR measures were 93.09% and 96.58% respectively. Our results are similar to the results of Chen *et al.* [9] regarding TPR and Dice measures (Fig. 4).

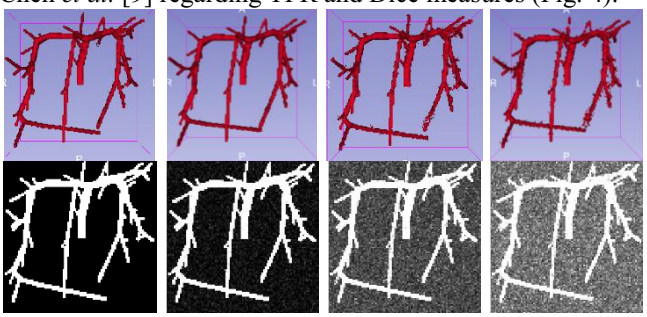

Fig. 4 – Typical Segmentation results (synthetic images). Top row: 3D view of the results. Bottom: MIP of the input images. From left to right, noise variances are 0%, 3%, 5% and 7%.

3.2. Clinical Data Segmentation

We compared the proposed method with conventional graph-cuts and fast-marching techniques. Regarding the fast-marching method, the results were not acceptable and it needed a large user-interaction to define seed points. In low-contrast CT images, the results leaked to the liver tissue. Concerning the graph-cuts algorithm, the results are shown in Fig. 5. The input images include normal, abnormal and low-contrast data. The results of the graph-cuts were obtained after smoothing and removing trivial objects. Compared to the graph-cuts method, our algorithm is automatic and does not need the tedious task of seed generation. We define seed points automatically in the proposed method. As it is shown in Fig. 5, our method does not label liver tissues as vessels. It preserves connectivity of the vessels and segments lower order branches better (Fig. 5). Since our method estimates the parameters of the data term locally, it takes into consideration variations of contrast media intensity. In the conventional graph-cuts algorithm, the data term parameters are obtained using high-contrast vessel. Thus, low-contrast vessels have a high value of data term and they are therefore considered as background voxels. Using the proposed method, extraction of lower branches is improved compared to Pock's method (Fig. 2)

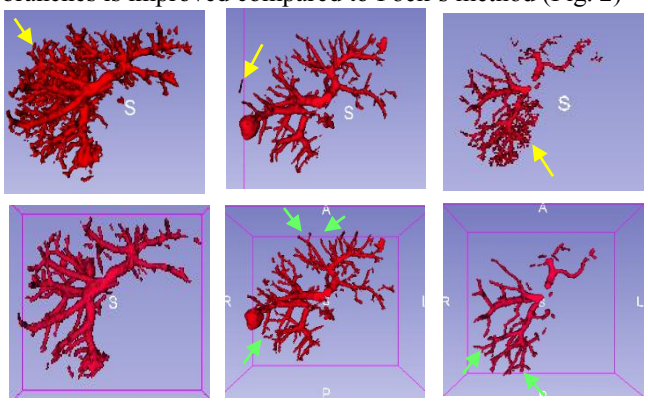

Fig. 5 – Top row: Segmentation results of the conventional graph-cuts. Bottom: Results of the proposed method. From left to right: Datasets are no. 3 (normal), no. 14 (abnormal) and no. 16 (low-contrast). Yellow arrows show non-vessel objects and green arrows show connectivity of the results.

We also define a mask to search for vessels using the output of Pock's method to decrease the run-time and memory requirements of the graph-cuts algorithm.

Regarding accuracy and sensitivity measures, our average results are 92.6% and 96.7% which are better than the results of Luu *et al.* [10] and Marcan *et al.* [6].

The run-time of our algorithm is 92 seconds for a typical data which is mainly for the Pock and skeletonization algorithms. Regarding conventional graph-cuts algorithm, it approximately took 20 seconds to segment vessels in a typical CT image. This figure excludes the time needed for seed generation by a user.

4. CONCLUSION AND FUTURE WORKS

In this paper, we proposed a segmentation method based on the graph-cuts algorithm. We calculated t-link weights using the proposed appearance models. Compared to recent researches, quantitative results of our method are comparable. Regarding the conventional graph-cuts technique, the proposed method is automatic and does not miss small/low-contrast vessels. We did not consider directional information of the vessels when we extracted medial axes. A solution is to isotropic resampling of the input image. It needs a large memory to process the corresponding graph matrix. Otherwise, we have to employ directional filters which can be considered as a future work.

In future, we plan to apply our method on more clinical datasets including both normal and pathological images.

5. REFERENCES

[1] S. Sherlock and J. Dooley, *Diseases of the liver and biliary system*. John Wiley & Sons, 2008.

[2] A. F. Frangi, W. J. Niessen, K. L. Vincken, and M. A. Viergever, "Multiscale vessel enhancement filtering," in *International Conference on Medical Image Computing and Computer-Assisted Intervention*, 1998, pp. 130–137.

[3] Y. Sato *et al.*, "Three-dimensional multi-scale line filter for segmentation and visualization of curvilinear structures in medical images," *Med. Image Anal.*, vol. 2, no. 2, pp. 143–168, 1998.

[4] Z. Zhai, M. Staring, and B. C. Stoel, "Lung vessel segmentation in CT images using graph cuts," in *SPIE Medical Imaging*, 2016, p. 97842K--97842K.

[5] P. R. Wankhede and K. B. Khanchandani, "Retinal blood vessel segmentation using graph cut analysis," in *Industrial Instrumentation and Control (ICIC), 2015 International Conference on*, 2015, pp. 1429–1432.

[6] M. Marcan, D. Pavliha, M. M. Music, I. Fuckan, R. Magjarevic, and D. Miklavcic, "Segmentation of hepatic vessels from MRI images for planning of electroporation-based treatments in the liver," *Radiol. Oncol.*, vol. 48, no. 3, pp. 267–281, 2014.

[7] L. Wang, C. Hansen, S. Zidowitz, and H. K. Hahn, "Segmentation and separation of venous vasculatures in liver CT images," in *SPIE Medical Imaging*, 2014, p. 90350Q--90350Q.

[8] L. Wang *et al.*, "Segmentation of hepatic arteries in multi-phase liver CT using directional dilation and connectivity analysis," in *SPIE Medical Imaging*, 2016, p. 97851P--97851P.

[9] Y. Cheng, X. Hu, J. Wang, Y. Wang, and S. Tamura, "Accurate vessel segmentation with constrained B-snake," *IEEE Trans. Image Process.*, vol. 24, no. 8, pp. 2440–2455, 2015.

[10] H. M. Luu, C. Klink, A. Moelker, W. Niessen, and T. van Walsum, "Quantitative evaluation of noise reduction and vesselness filters for liver vessel segmentation on abdominal CTA images," *Phys. Med. Biol.*, vol. 60, no. 10, p. 3905, 2015.

[11] S. Lu, H. Huang, P. Liang, G. Chen, and L. Xiao, "Hepatic vessel segmentation using variational level set combined with non-local robust statistics," *Magn. Reson. Imaging*, vol. 36, pp. 180–186, 2017.

[12] B. Chen, Y. Sun, and S. H. Ong, "Liver vessel segmentation using graph cuts with quick shift initialization," in *The 15th International Conference on Biomedical Engineering*, 2014, pp. 188–191.

[13] E. W. Dijkstra, "A note on two problems in connexion with graphs," *Numer. Math.*, vol. 1, no. 1, pp. 269–271, 1959.

[14] S. Esneault, C. Lafon, and J.-L. Dillenseger, "Liver vessels segmentation using a hybrid geometrical moments/graph cuts method," *IEEE Trans. Biomed. Eng.*, vol. 57, no. 2, pp. 276–283, 2010.

[15] A. H. Foruzan, R. A. Zoroofi, Y. Sato, and M. Hori, "A Hessian-based filter for vascular segmentation of noisy hepatic CT scans," *Int. J. Comput. Assist. Radiol. Surg.*, vol. 7, no. 2, pp. 199–205, 2012.

[16] T. Pock, C. Janko, R. Beichel, and H. Bischof, "Multiscale medialness for robust segmentation of 3d tubular structures," in *Proceedings of the Computer Vision Winter Workshop*, 2005, vol. 2005.

[17] T.-C. Lee, R. L. Kashyap, and C.-N. Chu, "Building skeleton models via 3-D medial surface axis thinning algorithms," *CVGIP Graph. Model. Image Process.*, vol. 56, no. 6, pp. 462–478, 1994.

[18] Y. Boykov and V. Kolmogorov, "An experimental comparison of min-cut/max-flow algorithms for energy minimization in vision," *IEEE Trans. Pattern Anal. Mach. Intell.*, vol. 26, no. 9, pp. 1124–1137, 2004.

[19] P. Jassi and G. Hamarneh, "Vascusynth: Vascular tree synthesis software," *Insight J.*, 2011.

[20] G. Hamarneh and P. Jassi, "VascuSynth: simulating vascular trees for generating volumetric image data with ground-truth segmentation and tree analysis," *Comput. Med. imaging Graph.*, vol. 34, no. 8, pp. 605–616, 2010.